

# Topography and Coating of Platinum Improve the Electrochemical Properties and Neuronal Guidance

Sabrina Schlie-Wolter,<sup>\*,†,‡</sup> Andrea Deiwick,<sup>†,‡</sup> Elena Fadeeva,<sup>‡</sup> Gerrit Paasche,<sup>§</sup> Thomas Lenarz,<sup>§</sup> and Boris N. Chichkov<sup>‡</sup>

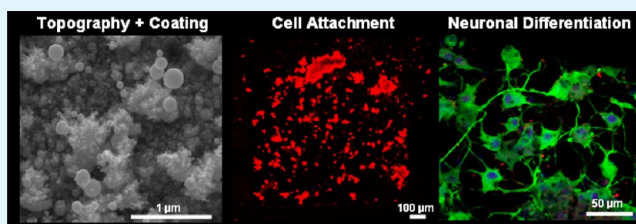
<sup>‡</sup>Laser Zentrum Hannover e.V., Hollerithallee 8, 30419 Hannover, Germany

<sup>§</sup>Department of Otolaryngology, Hannover Medical School, Carl-Neuberg-Strasse 1, 30625 Hannover, Germany

## Supporting Information

**ABSTRACT:** To improve neuronal-electrode interfaces, we analyzed the influence of surface topographies combined with coating on the electrochemistry of platinum and neuronal differentiation of PC-12 cells. Surface structuring on nanoscale was realized by femtosecond laser ablation. Additional coating with laminin (LA), collagen type I (COL) or poly-D-lysine (PDL) did not change the produced topography. We further demonstrated that impedance could be improved in all cases. The pre-requisites of differentiation — viability and attachment — were fulfilled on the topography. Cell attachment of non-differentiated and differentiated cells and their formation of focal adhesion complexes were even enhanced compared to unstructured platinum. However, without the nerve growth factor (NGF) no cellular outgrowth and differentiation were possible. The topography enabled cell elongation and reduced the amount of rounded cells, but less effective than coating. Differentiation was either comparable or increased on the structures when compared with unstructured coatings. For instance, microtubule associated protein (MAP2) was detected most on the topography alone. But a combination of surface structuring and coating had the strongest impact on differentiation: the usage of COL provoked best cell elongation and beta III tubulin expression, PDL best synaptophysin. LA-coating had no noteworthy effect. These findings point out that innovative electronic devices like cochlear implants include two aspects: (a) nanotopography to improve the transmission of electrical signals and neuronal attachment; and (b) an additional coating to stimulate neuronal differentiation.

**KEYWORDS:** surface modification, topography, nerve regeneration, neural prosthesis, electronic material



## 1. INTRODUCTION

One of the challenging key topics in biomedical research is devoted to the stimulation of nerve tissues or the recording of electrophysiological signals. Recent achievements of these electronic devices can find their application as neural prosthesis such as cochlear or retina implants or for the treatment of neurodegenerative diseases like Morbus Parkinson.<sup>1,2</sup>

From the technical point of view, such electronic devices require stable and low impedance in order to stimulate neuronal tissue.<sup>3</sup> Because of the demanded specifications, metallic conductors such as platinum, platinum iridium alloys, and titanium nitride are commonly used.<sup>4,5</sup> However, conductive polymers like poly(3,4-ethylenedioxythiophene) (PEDOT) were also shown to fulfil the desired properties.<sup>6</sup> To make electrodes more efficient, biological aspects related to neuron–electrode interactions became a matter of increasing interest. Therefore, materials have to be selected for their electrochemistry and compatibility with fabrication process, but also for neuronal guidance and stimulation. In that context, the formation of neuronal extensions and synapses on electrode surfaces — as signs for neuronal differentiation — were described to be the critical parameters.<sup>7</sup> Because cell differ-

entiation depends on external physical and chemical stimuli, electrode surface design has to be optimized in order to produce advanced electronic devices.<sup>8</sup>

A physiological relevant topography, that imitates the native environment of the cells, could potentially be utilized for directing diverse cell functions. By this means, cell proliferation, attachment, morphology, differentiation, orientation, or migration can be controlled.<sup>9–12</sup> However, it varies across the cell type, provided matrix, surface geometry, and feature dimensions. For instance, the differentiation of human and mouse mesenchymal stem cells or osteoprogenitor cells could be improved by nano-topography.<sup>13,14</sup> Interestingly, the topography alone can directly modulate stem cell differentiation.<sup>15</sup> The relation between topography and cell control is probably mediated by cell attachment: contributed by a mechanotransductive signaling of focal adhesion complexes, which regulate transcription factor activity, gene and protein expression.<sup>15</sup> But the underlying mechanism seems to be more

**Received:** November 26, 2012

**Accepted:** January 17, 2013

**Published:** January 17, 2013

complex, because stem cell differentiation is further dependent on cell morphology, cell density, and cell–cell-contacts.<sup>16</sup> Concerning neuronal interactions only little information is available. Cecchini et al.<sup>8</sup> demonstrated that PC-12 cells attach onto nanogrooves without additional coating and that dendrites orientate along the grooves. Rougher topographies and microsized spike structures promoted the attachment and formation of neuronal networks of primary neurons.<sup>17,18</sup> However, the improvement of neural–electrode interfaces requires a more detailed analysis of neuronal differentiation on the presented electrode.

Electrode optimization can be realized by material functionalization. Biological/chemical functionalization refers to surface coating with neuronal–stimulative adhesive peptides, growth or differentiation factors. Physical functionalization is based on the fabrication of defined surface topographies, nowadays realizable by recent developments in micro- and nanofabrication techniques. However, such work does not concern following topics: (a) how do surface topography and/or coating change the electrochemical properties of the electrode material; (b) do surface topography and/or coating affect neuronal attachment, morphology and differentiation? Providing answers to these questions was the aim of our study.

Our electrode material of choice is platinum (Pt) because of its widespread commercial usage. Surface structuring was realized by the use of femtosecond laser ablation. This technology has many advantages in comparison to others (e.g., lithography or chemical deposition). It enables contact-free and one step processing, which can be applied for machining of work pieces with complicated geometries. In comparison to long pulse lasers ultra-short laser processing is characterized by a higher spatial resolution, a high reproducibility, and the absence of side-effects like mechanical damages.<sup>19,20</sup> Surface coating was performed with laminin (LA), collagen type I (COL), poly-D-lysine (PDL), and COL-PDL.<sup>21</sup> Neuronal differentiation was verified with focus on PC-12 cell line (rat pheochromocytoma), which exhibit several neuronal characteristics following the treatment with nerve growth factor (NGF).<sup>22,23</sup> In addition to the characterization of the functionalized Pt surfaces with respect to impedance, we analyzed surface effects on cell viability, attachment, morphology, and differentiation.

## 2. MATERIALS AND METHODS

**2.1. Surface Structuring, Coating, and Characterization.** For our experiments, samples with a size of  $8 \times 8 \times 0.25 \text{ mm}^3$  were prepared from commercial platinum (Pt) foils with a purity of 99.99 % (Goodfellow, Germany). Prior to femtosecond laser surface treatment, all samples were cleaned with methanol. For structure fabrication, an amplified Ti:sapphire femtosecond laser system (Femtolasers Production GmbH, Austria) was used, which delivers linearly polarized sub-30 fs pulses at 800 nm at a repetition rate of 1 kHz.

The structures were generated by raster scanning a femtosecond laser beam across the sample using a laser fluence of  $7.7 \text{ J/cm}^2$ . Thereby,  $1 \times 1 \text{ mm}^2$  structured areas were manufactured in the middle of Pt samples, whereas marginal areas were left unstructured and served as control surfaces.

Before coating, structured Pt samples were sterilized under UV light for 1 h. A non-coated but structured sample served as an additional control. Using sterile stocking solutions, LA (in phosphate buffered saline PBS) and COL (in 0.02 N acetic acid) were coated with  $5 \mu\text{g/cm}^2$ , PDL (in water) with 0.1 mg/mL and COL-PDL 1:1. All reagents were given onto the entire Pt sample surface (structured and non-structured) for comparison. After incubating at  $37 \text{ }^\circ\text{C}$  for 1 h, the samples were washed with PBS three times. After processing, Pt

surfaces were visualized by scanning electron microscopy (SEM). To guaranty the quality of the produced surfaces, we visualized all used samples.

The electrochemical characterization of the samples was provided by impedance measurements. For that purpose, test platinum electrodes with the size of  $1 \times 2 \times 0.25 \text{ mm}^3$  were manufactured. The surface of  $2 \times 1 \text{ mm}^2$  was left free while remaining surfaces were insulated by using of MED-4234 silicone (NuSil Technology, USA). One test electrode was not structured and served as a counter electrode. Other Pt electrodes were structured using the same processing parameters as for the cell culture experiments. Test electrodes were connected by using of silicone-insulated 0.2 mm thick, 5 cm long Pt/Iridium wires. The measurement data were obtained using the structured electrode in countercurrent with the unstructured electrode, placed in 0.9 % physiological saline (Animed, Switzerland), with LCR HiTESTER 3522-50 (HIOKI, Japan). The electrical impedances were measured over a frequency range of 1 to  $1 \times 10^5 \text{ Hz}$  with sinusoidal current excitation ( $10 \mu\text{A}$ ).

**2.2. Cell Culture and Staining.** If not specified, all antibodies and agents were purchased from Sigma-Aldrich (Taufkirchen, Germany). PC-12 cells (DSMZ, Braunschweig, Germany) were cultivated in RPMI medium supplemented with 10 % horse and 5 % fetal bovine serum and antibiotics (Lonza, Basel, Switzerland). For differentiation, 100 ng/mL NGF was added. Concerning neuronal-surface interactions, three cell setups were used. The first setup was performed with pre-differentiated cells, which were cultivated with NGF-containing medium for six days beforehand. Then these cells were trypsinized and seeded onto the samples. Further culturing was performed with NGF-containing medium in order to analyze the ability to maintain the differentiation potential. The second setup consisted of non-differentiated cells, which were cultivated on the samples without NGF-containing medium. This setup further refers to control cells. To investigate whether the cells can differentiate on the samples directly, we cultivated non-differentiated cells on the samples with the addition of NGF. This third setup is named differentiated cells.

Cell viability was analyzed via calcein AM staining. Neuronal attachment was determined with respect to the formation of focal adhesion complexes via staining phosphorylated focal adhesion kinase (FAK p-Tyr<sup>397</sup>). The functionality of synapses was verified by the synaptic vesicle marker synaptophysin.<sup>23,24</sup> To identify microtubules of dendrites, neuronal beta III tubulin and microtubule associated protein (MAP2) were labelled. Beta III tubulin staining was further used to estimate the cell morphology.

After 48 h culturing of pre-differentiated cells and 5 days culturing of control and differentiated cells, the cells were fixed using 4 % paraformaldehyde dissolved in PBS for 20 min at  $4 \text{ }^\circ\text{C}$ . Following several washing steps with PBS, unspecific antibody binding was blocked by using 0.5 % bovine serum. Then, the primary antibodies incubated at  $4 \text{ }^\circ\text{C}$  overnight. After further washing steps, the secondary antibody and Hoechst 33342 for nucleus staining were added at  $37 \text{ }^\circ\text{C}$  for 1 h. All reagents were diluted in 0.3 % Triton-X 100 solution (in PBS). Images were recorded with a fluorescence microscope (Nikon, Düsseldorf, Germany).

**2.3. Quantification of Neuronal Viability, Attachment, Morphology and Differentiation.** The entire structured-coated surface was documented in comparison to the unstructured-coated surface aside and non-coated control. Except for the viability measurements all results were obtained from 50 cells per treatment.

To quantify the viability of pre-differentiated cells, we counted and normalized the number of calcein AM stained cells on the total cell number visualized by nucleus staining. The results are given as average in percent  $\pm$  s.e.m. (standard error of mean).

Cell morphology was classified with respect to cell elongation and cell size of beta III tubulin stained cells. For that purpose, ImageJ software was applied (<http://rsbweb.nih.gov/ij/>). A straight line was placed on the length and width of the entire cell body, each. Their ratio ( $\text{cell}_{\text{ratio}} = \text{cell}_{\text{length}} / \text{cell}_{\text{width}}$ ) enabled calculation of cell elongation  $\pm$  s.e.m.<sup>20</sup> Cells presenting a  $\text{cell}_{\text{ratio}}$  smaller than the value of 2 were defined as rounded cells. The amount of rounded cells

was summarized for each sample, normalized on the total analyzed cell number and given in percent. Additionally, the lengths of elongated cells with a  $\text{cell}_{\text{ratio}}$  bigger than the value of 2 was averaged and given in  $\mu\text{m} \pm \text{s.e.m.}$

Quantification of cell attachment, which referred to FAK staining, and cell differentiation via staining of beta III tubulin, MAP2 and synaptophysin were performed in the same manner according to the description in.<sup>25</sup> Using ImageJ software, a rectangle with  $3600 \text{ pixel}^2$  was placed on each cell and the single RGB colour channel could be classified using the colour channel that correlates with the staining of interest. Additionally, a rectangle of the same size was placed aside the cells of the same image to quantify the background signal for each image. Via abstracting the background signal from the cell signal, the relative mean fluorescence intensity for each staining could be estimated and be given as average  $\pm \text{s.e.m.}$

**2.4. Statistical Analysis.** To investigate whether statistical differences with respect to the differentiation markers (synaptophysin, beta III tubulin, MAP2), cell morphology (cell length and cell ratio) and focal adhesion complex (FAK p-Tyr<sup>397</sup>) occurred, Student's-t-test was applied with significance levels of  $p < 0.05$ ,  $p < 0.01$ , and  $p < 0.001$  for control, pre-differentiated, and differentiated cells each. In this connection the impact of the topography was analyzed by comparing the structured uncoated with the unstructured surfaces. To investigate the influence of the coating, we analyzed differences between the structured-uncoated surface with structured-coated surfaces.

### 3. RESULTS

**3.1. Nanostructures, Coating, and Impedance.** Laser-structuring of Pt resulted in a porous topography consisting of nano- and micro-scale cavities, nano protrusions, and micro-scale aggregates (Figure 1a). Additional coating of the

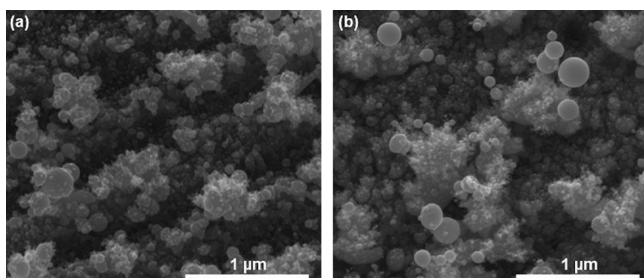
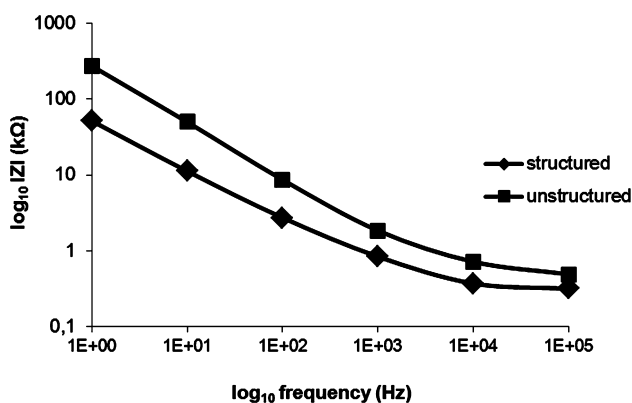


**Figure 1.** SEM images of structured platinum; comparison of (a) uncoated and (b) COL-coated.

topography did not change the surface features (Figure 1b). By comparing the laser-structured surface with a reference



electrode, we could find that structuring caused a marked reduction of electrical impedance in low-frequency range and exhibited nearly the same high-frequency impedance (Figure 2). Coating of the structured surfaces with COL, COL-PDL, and LA did not affect the electrical impedance significantly in comparison to structured and uncoated Pt (Figure 2).

**3.2. Cell Viability, Attachment, and Morphology.** Pre-differentiated PC-12 cells showed a high and comparable viability in contact with unstructured, structured and coated Pt. On the structured area, a viability of  $94.5 \% \pm 1.09$  was reached on the uncoated control, of  $93.54 \% \pm 1$  on LA, of  $93.49 \% \pm 0.88$  on COL, of  $93.17 \% \pm 2.27$  on PDL and of  $91.75 \% \pm 1.12$  on COL-PDL. On the unstructured area, the cells presented a viability of  $93.4 \% \pm 0.97$  on COL, of  $88.57 \% \pm 2.96$  on PDL and of  $92.57 \% \pm 1.54$  on COL-PDL. On the control and on LA, the cells attached only onto the structured area.

This finding was in accordance with a more detailed analysis of cell attachment focussing on FAK p-Tyr<sup>397</sup>, which is only detectable in cells when they are attached to the surface via ECM-integrin-binding.<sup>25</sup> Pre-differentiated and differentiated cells did not adhere on unstructured-uncoated and unstructured-LA-coated Pt (Figure 3). Control cells did not attach on

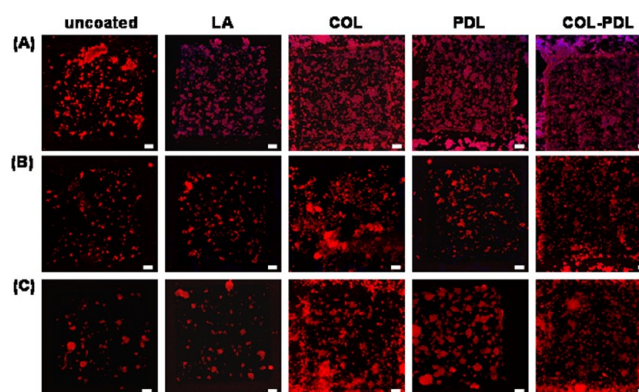


**Figure 3.** Attachment of (A) pre-differentiated, (B) control, and (C) differentiated PC-12 cells on structured Pt with different coatings (via FAK p-Tyr<sup>397</sup> staining (red); scale bars =  $100 \mu\text{m}$ ).

the unstructured material at all. Therefore, a statistical analysis between the uncoated structured and unstructured surface could not be carried out. To identify the impact of the

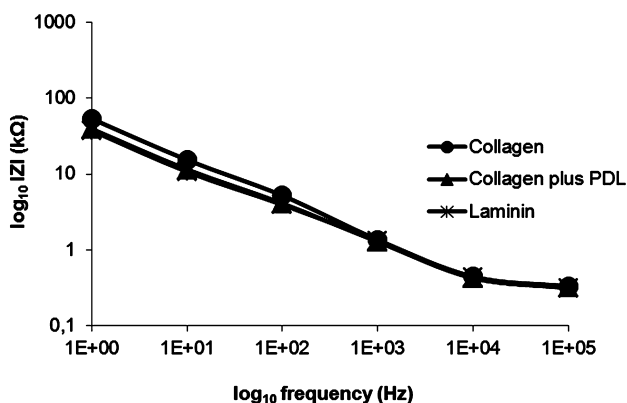


**Figure 2.** Impedance spectrum of unstructured Pt reference electrode and femtosecond laser-structured Pt (left); impedance spectrum of femtosecond laser structured Pt coated with COL, COL-PDL, and LA (right).



topography alone, the uncoated structured control surface had to be compared with unstructured COL-, PDL- and COL-PDL-coated surfaces as positive controls instead.

To get more insights, the degree of attachment was quantified (Figure 4). Concerning pre-differentiated cells the

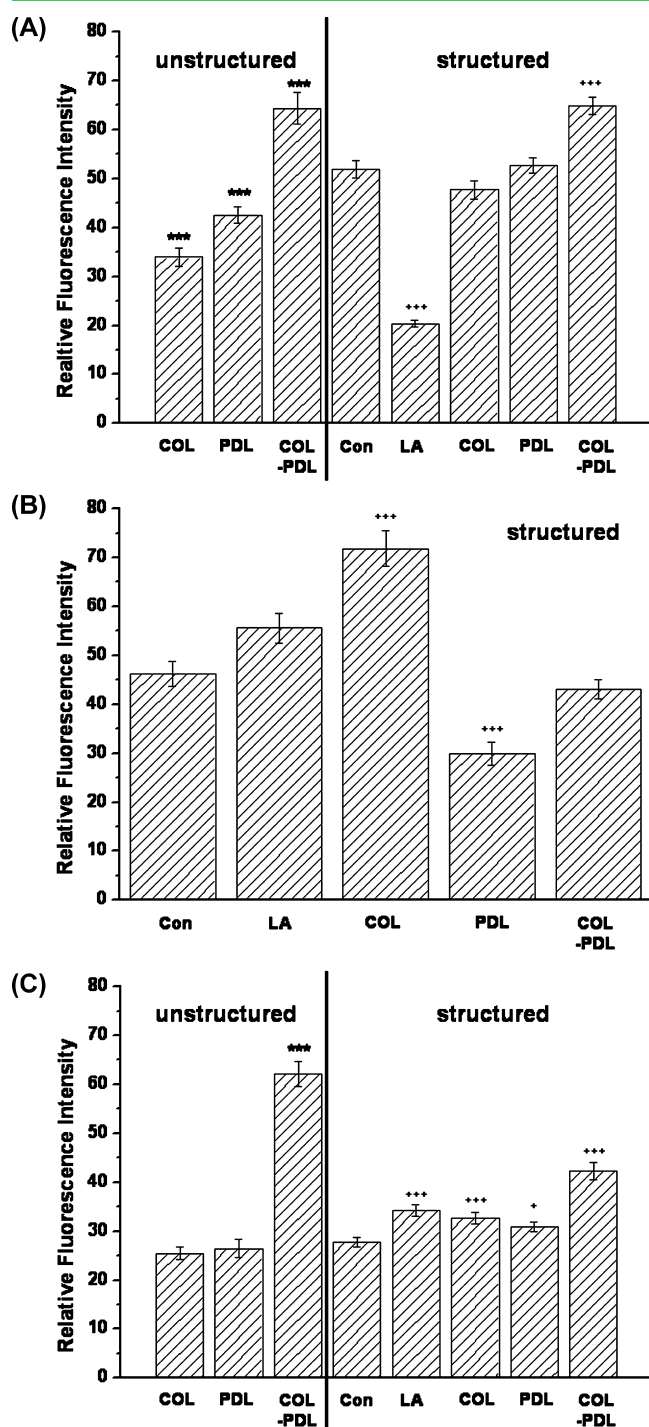


**Figure 4.** Quantification of PC-12 cell attachment onto structured and coated Pt surfaces after FAK Tyr<sup>397</sup> staining. The results are given as the mean relative fluorescence intensity  $\pm$  s.e.m. of 50 cells per treatment. (a) pre-differentiated; (b) control; (c) differentiated cells. Student's-t-test analysis:  $p < 0.05$  (\* or +),  $p < 0.01$  (\*\* or ++),  $p < 0.001$  (\*\*\*) or (+++), whereas \* describes the difference caused by topography, and + the difference caused by coating.

differences between the topography alone and positive controls were significant. In comparison to the structure, the attachment was significantly better on COL-PDL and significantly lower on COL and PDL. Focussing on differences caused by coating, it was found that the FAK value was significantly higher on COL-PDL, significantly lower on LA and similar on COL and PDL alone. Unstructured and structured COL-PDL had a comparable FAK value of about 64 (Figure 4a).

Differentiated cells also attached the best onto COL-PDL coating, in this connection better on unstructured Pt with an intensity of 62 than on structured with an intensity of 42 (Figure 4c). Concerning the uncoated structured control surface, FAK was significantly lower on the COL-PDL unstructured area, but similar on the other unstructured coatings. In comparison to the control, all FAK values were significantly higher on the coated structured surfaces.

Control cells did not attach to the unstructured surfaces at all (Figure 3). The topography alone enabled attachment. Concerning the structured area, the order was COL with a relative fluorescence intensity of 71 followed by LA > control = COL-PDL > PDL (Figure 4b). In comparison to the control surface, the effects of COL and PDL were significant.

Cell morphology was classified with respect to cell elongation, amount of rounded cells and cell length of elongated cells with cell<sub>ratio</sub>s bigger than 2 (see Table 1 in the Supporting Information). On all presented coatings control cells were rounded on the structures, while no cells attached on the unstructured area (Figure 3). The cell<sub>ratio</sub> was comparable on all treatments with a value of about 1.16–1.22.

The impact of the topography and coating on cell morphology of pre-differentiated cells basically followed the order COL > COL-PDL > PDL > structured control > LA. Concerning the length of the cells, this order was slightly shifted to COL > PDL > COL-PDL > control when the effects of the topography were considered alone. In a sum, the topography alone did not increase the cell<sub>ratio</sub> and length of elongated cells. Both parameters were even significantly smaller. On the control the amount of rounded cells was the highest with 90%, whereas it was the lowest on COL of 51% on the unstructured and comparably 48% on the structured surface. Additionally, the effects of the coating like COL were more pronounced, when it was coated on unstructured Pt. For instance, the length on unstructured COL of about 70  $\mu\text{m}$  was reduced to about 43  $\mu\text{m}$  on COL-structured surfaces and to 26  $\mu\text{m}$  on the structured control. The differences between the control and COL or COL-PDL were significant.

The same order starting with COL was also observed for differentiated cells. Coating was significantly more efficient with respect to cell elongation, length and reduced amount of rounded cells than the topography alone. The cells were significantly longer on the positive unstructured controls. Only the results for PDL-coating were similar with the control. However, a combination of topography and coating induced comparable values like for the unstructured coatings. For instance, lengths of 61  $\mu\text{m}$  on unstructured and 62  $\mu\text{m}$  on structured COL-surfaces were measured. But cell length was even higher on COL-PDL. COL further reduced the amount of rounded cells from 80% on the control to 44% on the structure and 38% on the unstructured area.

In general, COL-coating provoked single cell attachment and cellular extensions instead of the formation of aggregates independently from the topography. On the other coatings and

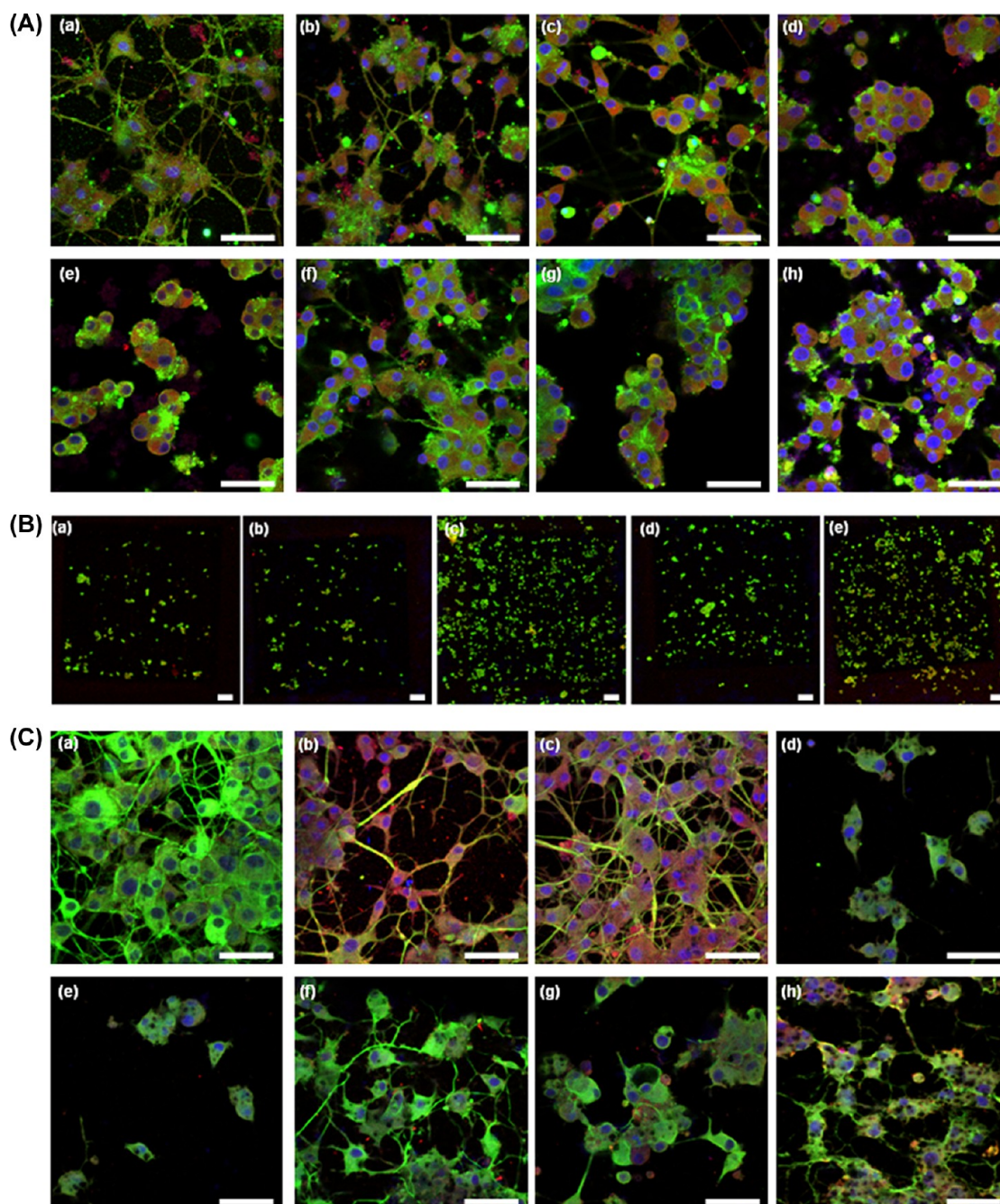


**Figure 5.** Fluorescence images of specific neuronal markers: (A) pre-differentiated PC-12 cells with MAP2 (green) and FAK (red) staining: (a–c) unstructured, (d–h) structured Pt; (d) control, (e) LA, (a, f) COL, (b, g) PDL, (c, h) COL-PDL. (B) control PC-12 cells with synaptophysin (green) and MAP2 (red) staining on structured Pt: (a) control, (b) LA, (c) COL, (d) PDL, (e) COL-PDL. (C) Differentiated PC-12 cells with beta III tubulin (green) and FAK (red) staining: (a–c) unstructured, (d–h) structured Pt; (d) control, (e) LA, (a, f) COL, (b, g) PDL, (c, h) COL-PDL. ((A, C) scale bars = 50  $\mu\text{m}$ ; (B) scale bars = 100  $\mu\text{m}$ .)

on the control, the cells formed aggregates and no cellular extensions; last point except for COL-PDL. (Figure 5)

**3.3. Neuronal Differentiation.** Neuronal differentiation was verified with focus on beta III tubulin, MAP2 and synaptophysin. Figure 5 reveals that PC-12 cells expressed the markers on all functionalized surfaces. However, the extent of the markers was dependent on the surface and culture condition (see Table 2 in the Supporting Information). All markers were quantified with the help of the relative fluorescence intensity, which referred to the corresponding staining.

For the control cells no detection of the markers on the unstructured surfaces was possible since there was no cell attachment (Figure 3). Therefore, the role of the topography alone could not be characterized. Concerning the coating effects it was found, that COL had a significant impact on beta III tubulin with a value of 80.96 followed in a similar manner by the control surface with a value of 60, LA and COL-PDL. The value on PDL was significantly lower than the control. However, coating did not enhance MAP2. In comparison to the control with a value of about 32, it was even significantly



reduced by PDL and COL. At the same time, all coatings significantly increased the amount of synaptophysin.

A statistical analysis revealed that the topography affects the differentiation of pre- and differentiated cells. Pre-differentiated cells expressed significantly more beta III tubulin on PDL and COL-PDL, but had a similar value on COL and the structured uncoated control with about 39. For differentiated cells this marker was significantly the highest on the COL-coated surface with a value of 74, followed by COL-PDL and the structured uncoated control. The value for the PDL-coated surface was significantly lower than on the Pt nanostructures. Concerning MAP2 it was found that the topography alone significantly enhanced its expression for pre-differentiated cells in all cases. On structured Pt differentiated cells presented either a comparable value or significant higher value when compared with the positive controls verified by a fluorescence intensity of 26.71 on the control structure and 12.33 on PDL-unstructured. Synaptophysin detection followed the order PDL > COL > structured control > COL-PDL with significant differences for pre-differentiated cells. Differentiated preferred COL- and COL-PDL-coated surfaces significantly, but its control value of 42.6 was comparable on PDL-coating.

To analyze the coating effects, we used the structured uncoated control for comparison. Pre-differentiated cells presented significantly more beta III tubulin on LA and PDL, while the others coatings were similar to the control with a value of 38.62. Differentiated cells had significantly more beta III tubulin on all coatings than on the control with 45.28. The amount of MAP2 was significantly the highest on the control for pre-differentiated cells with 89.73. For differentiated cells the effects were also significant except for COL-PDL. However, on PDL MAP2 was significantly higher, on COL- and LA-coating significantly lower than the control value of 26.71. For both cell setups, PDL-coating had the strongest and significant impact on synaptophysin. On the other coatings the values were similar to the control with 76.72 for pre-differentiated and 42.6 for differentiated cells, respectively.

#### 4. DISCUSSION

Platinum is the material of choice for neuroprosthetic devices, because of its corrosion resistance, biocompatibility, electrochemical properties, and appropriateness as implantable electrodes.<sup>26</sup> But currently, many applications need an improved selective stimulation of neuronal tissue and, hence, reduced size of stimulation electrodes. This, in turn, requires a higher stimulation current density, which leads to electrode corrosion and injury of the surrounding tissue.<sup>27</sup> To overcome this problem, one approach deals with surface structuring. By this means, the effective electrode surface can be increased significantly, and therefore, surface-dependent electrochemical properties can be improved.<sup>28</sup> In the past, mainly electrodeposition out of an electrolyte solution was applied to increase the effectiveness of platinum electrode surfaces. The deposited platinum film was called “platinum black” because of strong light absorption on its very rough surface. The impedance of “platinum black” electrodes decreases significantly.<sup>29</sup> However, the biocompatibility of such electrodes was problematic. In this regard surface structuring by ultra short pulse lasers is a more beneficial approach. It enables electrode processing in one step without additional chemicals. A large variety of surface features such as lines, holes, self-organized spikes, ripples, or micro- and nanoscaled roughness can be fabricated in almost all solid materials.<sup>12,19,20,30</sup>

In this study, a porous structure consisting of nano- and microscale cavities, nano protrusions, and micro-scale aggregates was generated on the Pt surfaces. (Figure 1a) These surface features were already described to suppress fibroblast proliferation.<sup>31</sup> To have a first insight on the influence of surface modifications on electrochemical properties, impedance spectra of unstructured and structured test electrodes were measured in the range of 1 to  $1 \times 10^5$  Hz. As shown in Figure 2, structuring leads to marked reduction of electrical impedance in low-frequency range and exhibit nearly the same high-frequency impedance. This resembles the impedance spectroscopic characteristics of “black platinum”.<sup>29</sup>

Beside the topographical functionalization of biomaterials, surface coating with respect to biological-chemical functionalization is also widely used. However, a combination of surface structuring and coating is hardly described in literature. First to be mentioned is that surface coating did not negatively affect the laser-generated topography itself (Figure 1b). Concerning impedance measurements, it was found that the reduced impedance values caused by topography were not significantly changed by additional coating (Figure 2). It can be concluded that structuring combined with coating enables the production of technically improved Pt.

Cell viability and attachment to the surface are basic requirements for a successful differentiation. Quantification of calcein AM staining revealed that surface structuring and coating did not cause toxic effects on the cells. But differences in cell attachment were observed (Figure 3). On unstructured and uncoated Pt no cell attachment was possible. Non-differentiated PC-12 cells are suspension cells, which require NGF and a specific surface coating for attachment. Interestingly, they were able to attach onto the structured Pt even without coating and NGF. The fact that surface structuring enhances cell attachment was also documented for micro-structured topographies.<sup>18</sup> Since the presence of surface roughness increases the surface area, it can be concluded that the correlated increased cell contact area improves attachment via ECM adsorption and cell binding.<sup>31</sup> Additionally, the extent of focal adhesion complexes was quantified with focus on phosphorylated FAK Tyr<sup>397</sup>, which is only expressed in cells, when they are bonded to the surface via ECM-integrins (Figure 4).<sup>25</sup>

The formation of focal adhesion complexes was enhanced by the topography, which supports the findings of previous studies.<sup>32</sup> Coating alone also affected cell attachment. Pre- and differentiated cells adhered onto COL-, PDL-, and with the highest extent on COL-PDL-coated unstructured Pt, but not on LA-coated or uncoated Pt surfaces (Figure 5a, c). The cells also preferred structured COL-PDL-coated Pt. In what manner the topography influences or may enhance the adsorption of the coating material, cannot be answered.

Because of the well-described outside-in signaling cascades, it can be concluded that attachment initiates cell differentiation and the formation of dendrites, which are a pre-requirement for functional synapses.<sup>32</sup> Additionally, cell elongation and the formation of dendrites are the strongest signs for neuronal differentiation.<sup>33</sup> Addressing the impact of the topography, unstructured coatings with COL, PDL, and COL-PDL were considered as positive controls for comparison. However, a clear correlation between the observed improved attachment on the topography and therefore, improved cell responses could not be addressed. Without NGF-conditioned medium no control cells could elongate. But the order of the cell<sub>ratios</sub> and

FAK values was similar (see Table 1 in the Supporting Information, Figure 4b). By adding NGF to the medium, cell elongation on the uncoated structured surface was possible. Here, the correlation between the FAK findings and morphology parameters could not be repeated (see Table 1 in the Supporting Information, Figure 4a and c). On the uncoated structure pre-differentiated cells were more rounded, shorter, and presented a smaller  $cell_{ratio}$  than cells that differentiated directly. Pre- and differentiated cells expressed similar levels of the neuronal markers on the uncoated topography when compared with the positive controls (Tab. 2; Supporting Information). MAP2 was even significantly increased on the structure for pre-differentiated cells. It can be concluded that the PC-12 are able to differentiate on the structured surface.

Addressing the functionality of the coating, the uncoated structured area was used for comparison. The  $cell_{ratio}$  of control cells was not improved by coatings. Adding NGF to the medium, cell elongation took place – but it was further enhanced by the coatings. The biggest impact on cell elongation had a coating with COL (see Table 1 in the Supporting Information). For the control cells, beta III tubulin was detected most on COL, synaptophysin on PDL, and MAP2 on COL-PDL, which was similar to the uncoated control surface (see Table 2 in the Supporting Information).

However, because PC-12 control cells did not elongate (see Table 1 in the Supporting Information), these results did not identify a successful stimulation of differentiation – neither by the topography nor by the coating. Differentiation only occurred in the presence of NGF-containing medium, but its extent was dependent on the presented surface design. Beta III tubulin was less detectable on the uncoated topography than on the coatings of pre- and differentiated cells. Concerning the coatings, COL had the strongest impact on beta III tubulin. This finding is in accordance with the highest cellular outgrowth on COL (see Table 1 in the Supporting Information), because this marker characterizes the formation of dendrites. On the contrary, MAP2 and synaptophysin were comparable or significantly increased for these cells on the topography alone. PDL-coating was found to be most important for synaptophysin of pre- and differentiated cells and also for MAP2 for differentiated cells. Cell morphology and differentiation was less dependent on the presence of LA. Even though LA as a component of the basement membrane plays a crucial role in developing and maturing the central nervous system, it rather stimulates cell aggregation than neurite outgrowth (Figure 3).<sup>21,24,35</sup>

The synergic effect between neurotrophic stimuli and ECM components was extensively studied in.<sup>34,36</sup> Here, we can differentiate between COL-PDL being most important for focal adhesion complexes, COL being most important for cell elongation and beta III tubulin, and PDL being most important for synaptophysin. It was described that beside the mechanical stability and cell binding capability, the ECM also exhibits a storage side for active neurotrophic factors like NGF. They further supposed that material coating with the ECM motivates cells to attach, which we confirmed in Figures 2 and 3, which thereby increases the probability of interactions between their NGF-receptor called tropomyosin kinase and NGF. Therefore, the increase of surface area by surface structuring may result in improved cell–NGF interactions supported by the mechanical stability of the enhanced focal adhesion complex formation.

## 5. CONCLUSIONS

The here demonstrated combination of surface topography and coating of platinum by laminin (LA), collagen type I (COL) or poly-D-lysine (PDL) has provided several advantages for future neuronal biomedical applications: (a) ultra short pulse laser ablation offers a controlled surface-patterning on nanometer scale, whereas the structure features stay persistent when additionally coated; (b) the structures improve impedance because of an increased surface area, which is not negatively affected by coating; (c) the modifications of platinum are not cytotoxic; (d) the topography enhances cell attachment significantly, but topography and coating do not stimulate neuronal differentiation; (e) neuronal differentiation requires NGF, but its extent correlates with the presented coating and topography: a combination of topography and coating had the strongest impact.

## ■ ASSOCIATED CONTENT

### Supporting Information

This material is available free of charge via the Internet at <http://pubs.acs.org>.

## ■ AUTHOR INFORMATION

### Corresponding Author

\*Phone: +49 511 2788-303. Fax: +49 511 2788-100. E-mail: [s.schlie@lzh.de](mailto:s.schlie@lzh.de).

### Author Contributions

†These authors contributed equally

### Notes

The authors declare no competing financial interest.

## ■ ACKNOWLEDGMENTS

This work was partly supported by the German Research Foundation, DFG SFB599 “Sustainable Bioresorbing and Permanent Implants of Metallic and Ceramic Materials” (subproject T2) and BMBF-project REMEDIS. The authors thank Prof. Dr. A. Ngezahayo (Institute of Biophysics, Leibniz University Hannover, Germany) for the usage of fluorescence microscope.

## ■ REFERENCES

- (1) Gosselin, B. *Sensors* **2009**, *11*, 4572–4597.
- (2) Eusebio, A.; Thavathasan, W.; Gaynor, L. D.; Poghosyan, A.; Bye, E.; Foltynie, T.; Zrinzo, L.; Ashkan, K.; Aziz, T.; Brown, P. *J. Neurol. Neurosurg. Psych.* **2011**, *82* (5), 869–873.
- (3) Reich, U.; Mueller, P. P.; Fadeeva, E.; Chichkov, B. N.; Stoeber, T.; Fabian, T.; Lenarz, T.; Reuter, G. *J. Biomed. Mater. Res. Part B: Appl. Biomater.* **2008**, *87B*, 146–153.
- (4) Rose, T. L.; Robblee, L. S. *IEEE Trans. Biomed. Eng.* **1990**, *199037*, 1119–20.
- (5) Weiland, J. D.; Anderson, D. J.; Humayun, M. S. *IEEE Trans. Biomed. Eng.* **2002**, *49*, 1574–79.
- (6) Cogan, S. F.; Peramunage, D.; Smirnov, A.; Ehrlich, J.; McCreery, D. B.; Manoonkitiwongsa, P. S. *Mater. Res. Soc. Meet. Boston* **2007**, 26–30.
- (7) Bieberich, E.; Guiseppi-Elie, A. *Biosens. Bioelectron.* **2004**, *19*, 923–931.
- (8) Cecchini, M.; Bumma, G.; Serresi, M.; Beltram, F. *Nanotechnology* **2007**, *18*, S05103.
- (9) Flemming, R. G.; Murphy, C. J.; Abrams, G. A.; Goodman, S. L.; Nealey, P. F. *Biomaterials* **1999**, *20*, 573–588.
- (10) Lim, J. Y.; Donahue, H. J. *Tissue Eng.* **2007**, *13* (8), 1879–1891.
- (11) Liu, H.; Webster, T. J. *Biomaterials* **2007**, *28*, 354–369.

- (12) Schlie, S. *Selective Cell Control for Biomedical Applications: Impact of Laser-Fabricated 3D Scaffolds and Surface Topographies*; Südwestdeutscher Verlag für Hochschulschriften: Saarbrücken, Germany, 2010.
- (13) Bettinger, C. J.; Langer, R.; Borenstein, J. T. *Angew. Chem., Int. Ed.* **2009**, *54*, 5406–5415.
- (14) Dellatore, S. M.; Garcia, A. S.; Miller, W. M. *Curr. Opin. Biotechnol.* **2008**, *19* (5), 534–540.
- (15) McNamara, L. E.; McMurray, R. J.; Biggs, M. J. P.; Kantawong, F.; Oreffo, R. O. C.; Dalby, M. J. *Tissue Eng.* **2010**, 120623 (13pp).
- (16) Peng, R.; Yao, X.; Cao, B.; Tang, J.; Ding, J. *Biomaterials* **2012**, *33*, 6008–6019.
- (17) Cyster, L. A.; Parker, K. G.; Parker, T. L.; Grant, D. M. *Biomaterials* **2004**, *25*, 97–107.
- (18) Papadopoulou, E. L.; Samara, A.; Barberoglou, M.; Manousaki, A.; Pagakis, S. N.; Anastasiadou, E.; Fotakis, C.; Stratakis, E. *Tissue Eng., Part C* **2010**, *16* (3), 497–502.
- (19) Fadeeva, E.; Schlie, S.; Koch, J.; Chichkov, B. N. *J. Adhes. Sci. Technol.* **2010**, *24*, 13–14.
- (20) Schlie, S.; Fadeeva, E.; Koch, J.; Ngezahayo, A.; Chichkov, B. N. *J. Biomater. Appl.* **2010**, *25* (3), 217–233.
- (21) Keshmirian, J.; Bray, G.; Carbonetto, S. *J. Neurocytol.* **1989**, *18*, 491–504.
- (22) Klesse, L. J.; Meyers, K. A.; Marshall, C. J.; Parada, L. F. *Oncogene* **1999**, *18*, 2055–2068.
- (23) Hans, A.; Syan, S.; Crosio, C.; Sassone-Corsi, P.; Brahic, M.; Gonzalez-Dunia, D. *J. Biol. Chem.* **2001**, *276* (10), 7258–7265.
- (24) Wheeler, T. C.; Chin, L.-S.; Li, Y.; Roudabush, F. L.; Li, L. *J. Biol. Chem.* **2002**, *277* (12), 10273–10282.
- (25) Schlie, S.; Gruene, M.; Dittmar, H.; Chichkov, B. N. *Tissue Eng., Part C* **2012**, DOI: 10.1089/ten.tec.2011.0635.
- (26) Geddes, L. A.; Roeder, R. *Ann. Biomed. Eng.* **2003**, *31*, 879–890.
- (27) Cogan, S. F. *Annu. Rev. Biomed. Eng.* **2008**, *10*, 275–309.
- (28) Kovacs, G. T. A. In *Enabling Technologies for Cultured Neural Networks*; Stenger, D. A., McKenna, T. M., Eds.; Academic Press: New York, 1994; pp 121–165.
- (29) Stieglitz, T. In *Neuroprosthetics: Theory and Practice*; Horch, K. W., Dhillon, G., Eds.; Series on Bioengineering & Biomedical Engineering; World Scientific: Singapore, 2004; Vol. 2, pp 475–516.
- (30) Vorobyev, A.; Guo, V. *COLA 2007: 9th International Conference on Laser Ablation*; Tenerife, Spain, ; Instituto de Óptica "Daza de Valdes", CSIC: Madrid, 2007.
- (31) Fadeeva, E.; Schlie, S.; Koch, J.; Chichkov, B. N.; Vorobyev, A. Y.; Guo, C. In *Contact Angle, Wettability and Adhesion*; Mittal, K. L., Ed.; Brill: Leiden, The Netherlands, 2009; Vol. 6, pp 163–171.
- (32) Ferrari, A.; Cecchini, M.; Dhawan, A.; Micera, S.; Tonazzini, I.; Stabile, R.; Pisognano, D.; Beltram, F. *Nano Lett.* **2011**, *11*, 505–511.
- (33) Lamoureux, P.; Steel, V. L.; Regal, C.; Adgate, L.; Buxbaum, R. E.; Heidemann, S. R. *J. Cell Biol.* **1990**, *110*, 71–79.
- (34) Achyuta, A. K. H.; Cieri, R.; Unger, K.; Murthy, S. K. *Biotechnol. Prog.* **2009**, *25*, 227–234.
- (35) Heiduschka, P.; Romann, I.; Ecken, H.; Schöning, M.; Schuhmann, W.; Thanos, S. *Electrochim Acta* **2001**, *47*, 299–307.
- (36) Schwarz, M. A.; Mitchell, M.; Emerson, D. L. *Cell Growth Diff.* **1990**, *1*, 313–318.